# Early Age Response of 3D Printed Systems Evaluated Using Analytical Models and Digital Image Correlation

**Narayanan Neithalath**

Professor

School of Sustainable Engineering and the Built Environment
Arizona State University
Narayanan.Neithalath@asu.edu
http://neithalath.engineering.asu.edu

**Avinaya Tripathi**

School of Sustainable Engineering and the Built Environment
Arizona State University

**Sooraj Nair**
USG Corporation

Presented at the ACI Spring Convention, Orlando, March 2022

# Printable cement-based materials

- 3D printing by layered extrusion
- Concrete soft enough to be extruded and to intermix with the previous layer
- Support its own weight and the weight of the superimposed layer
  - “Finite” waiting time between layers
  - Yield stress change from layer to structure
  - Rate of build up
  - Operation time


# Fresh state concerns

- Extrudability and Buildability (Printability)
- Open time - its influence on pumping and extrusion;
- Setting and layer cycle-time - its influence on vertical build rate;
- **Deformation of material as successive layers are added;**
- Rheology measurements - its importance to quality control

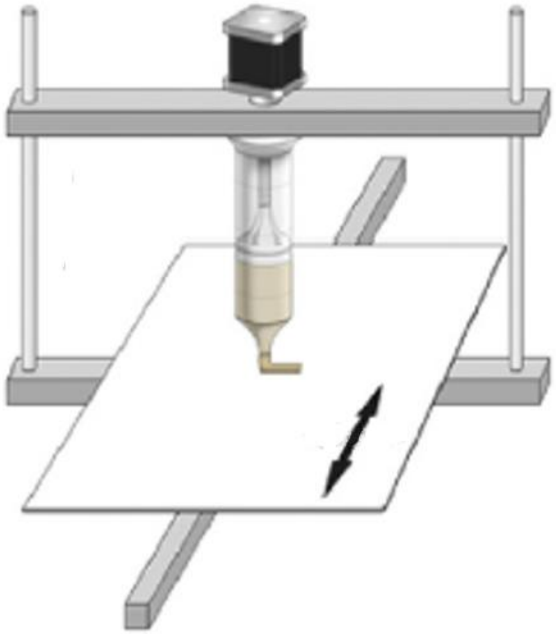

# Buildability of 3D printed systems

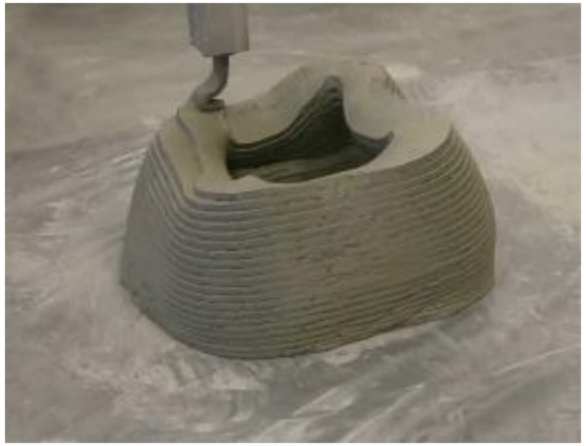


Suiker et al. 2020

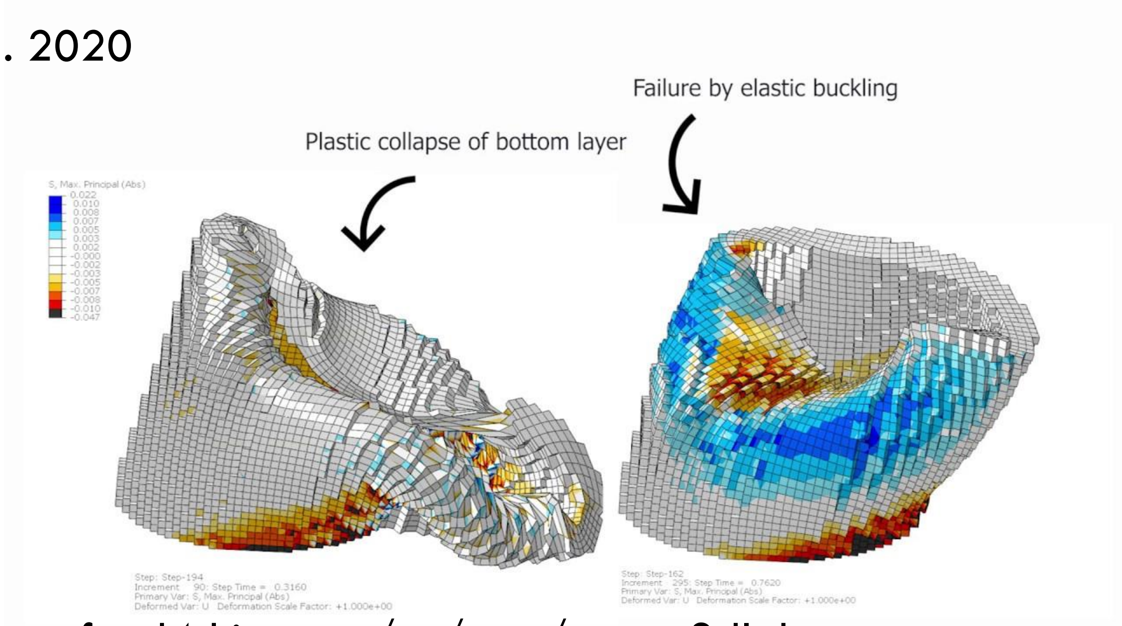


https://www.food4rhino.com/en/app/concre3dlab

# Overview

- Analytical model for buildability
  - Considering material property development, stepwise stress growth during printing, and failure modes
  - Verification using multiple print geometries
- Digital image correlation on fresh printed samples
  - Determining a failure initiation height, that is lower than the actual failure height
  - Predictive modes of failure through strain growth

# Formulating an analytical model

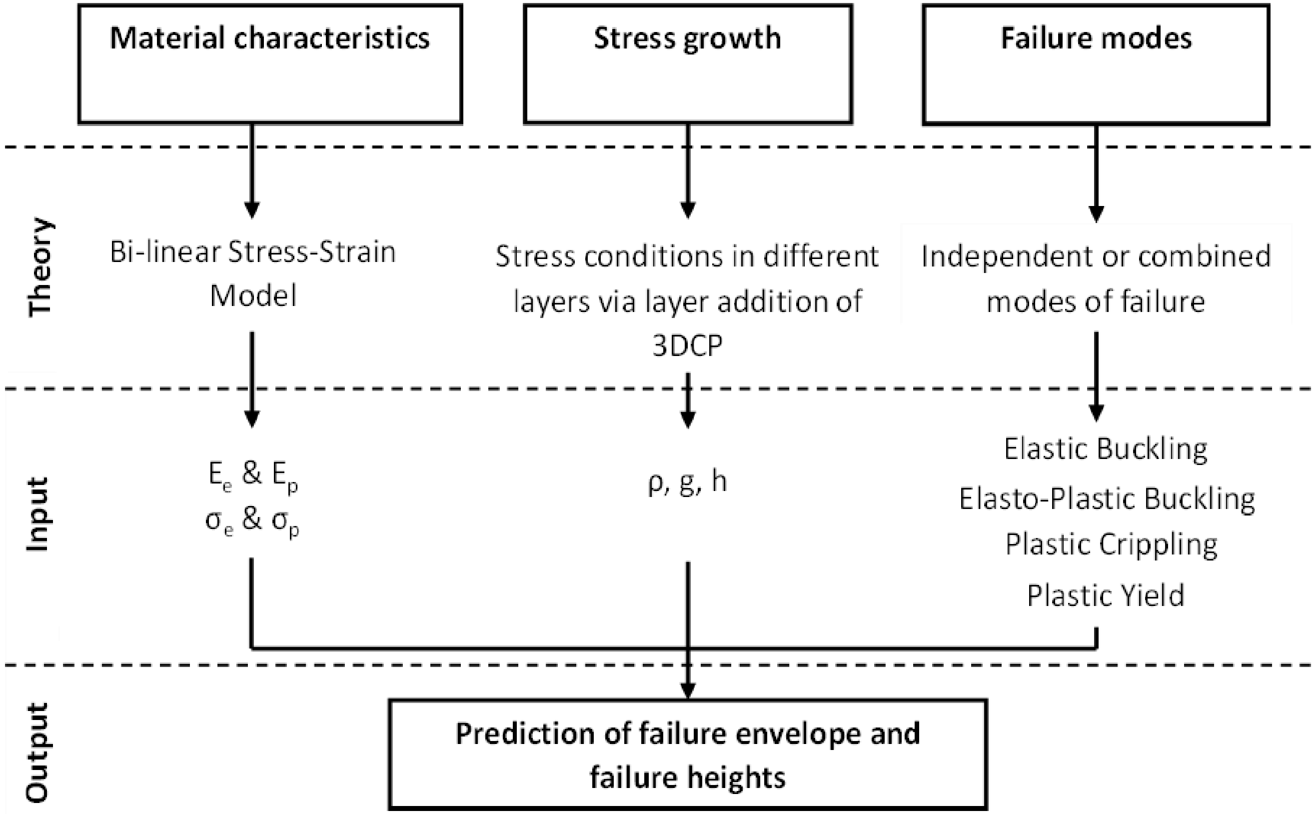


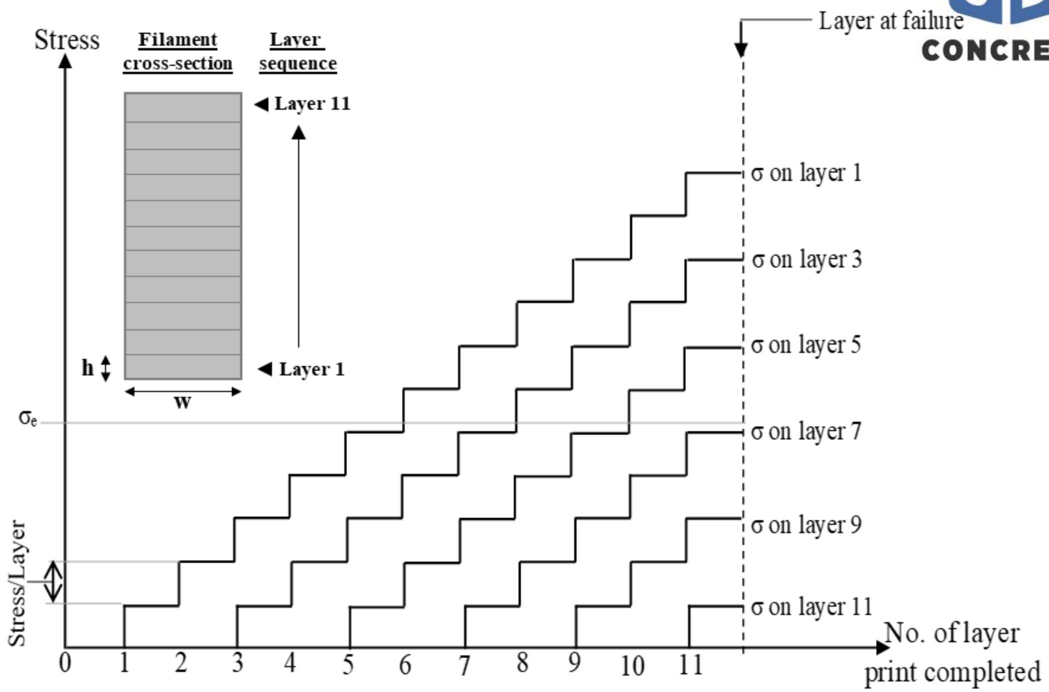


Stress growth in layers, with subsequent later deposition

$$Stress\ per\ layer = \frac{Filament\ Weight}{Filament\ Area} = \frac{\rho V g}{A} = \frac{\rho (A \times h) g}{A} = \rho \times h \times g$$

# Stress-strain response and stress growth

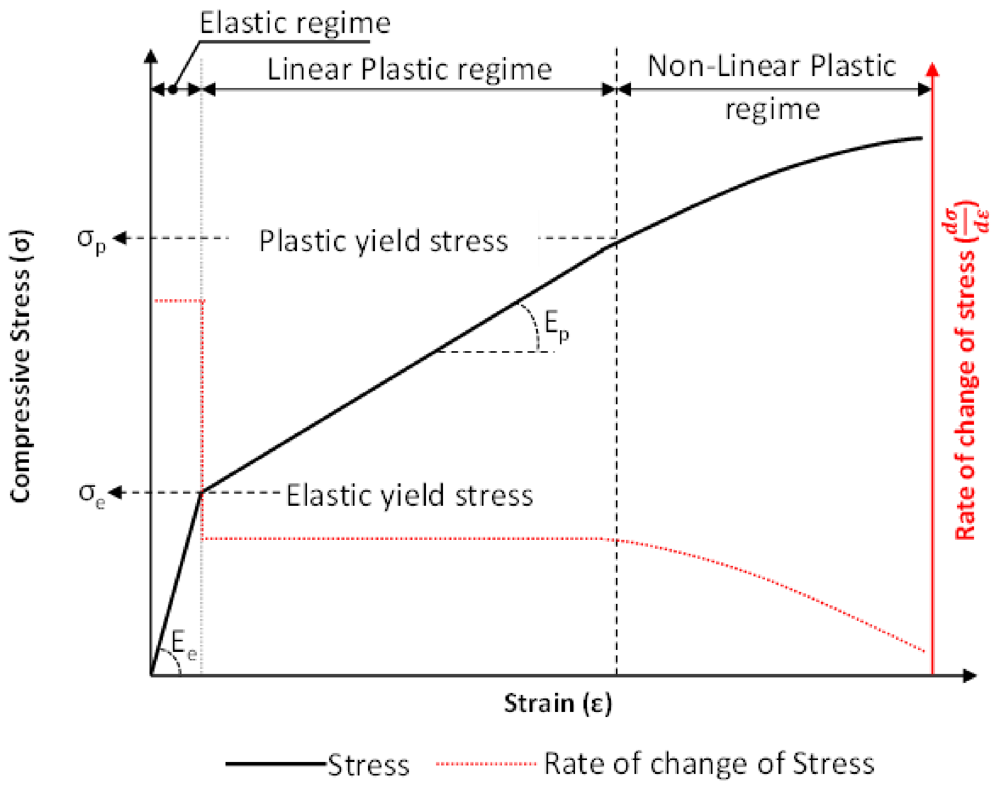


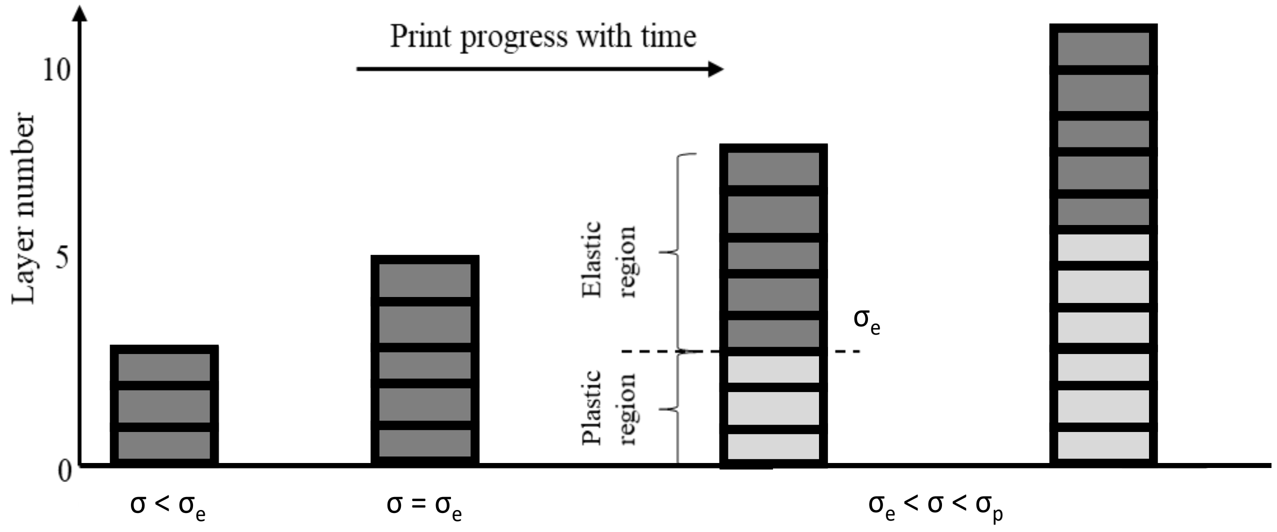


Layers experiencing stresses lower than the elastic yield stress (dark) and greater than the elastic yield stress (light); $\sigma$ is the stress on the bottommost layer of the print

# Failure modes

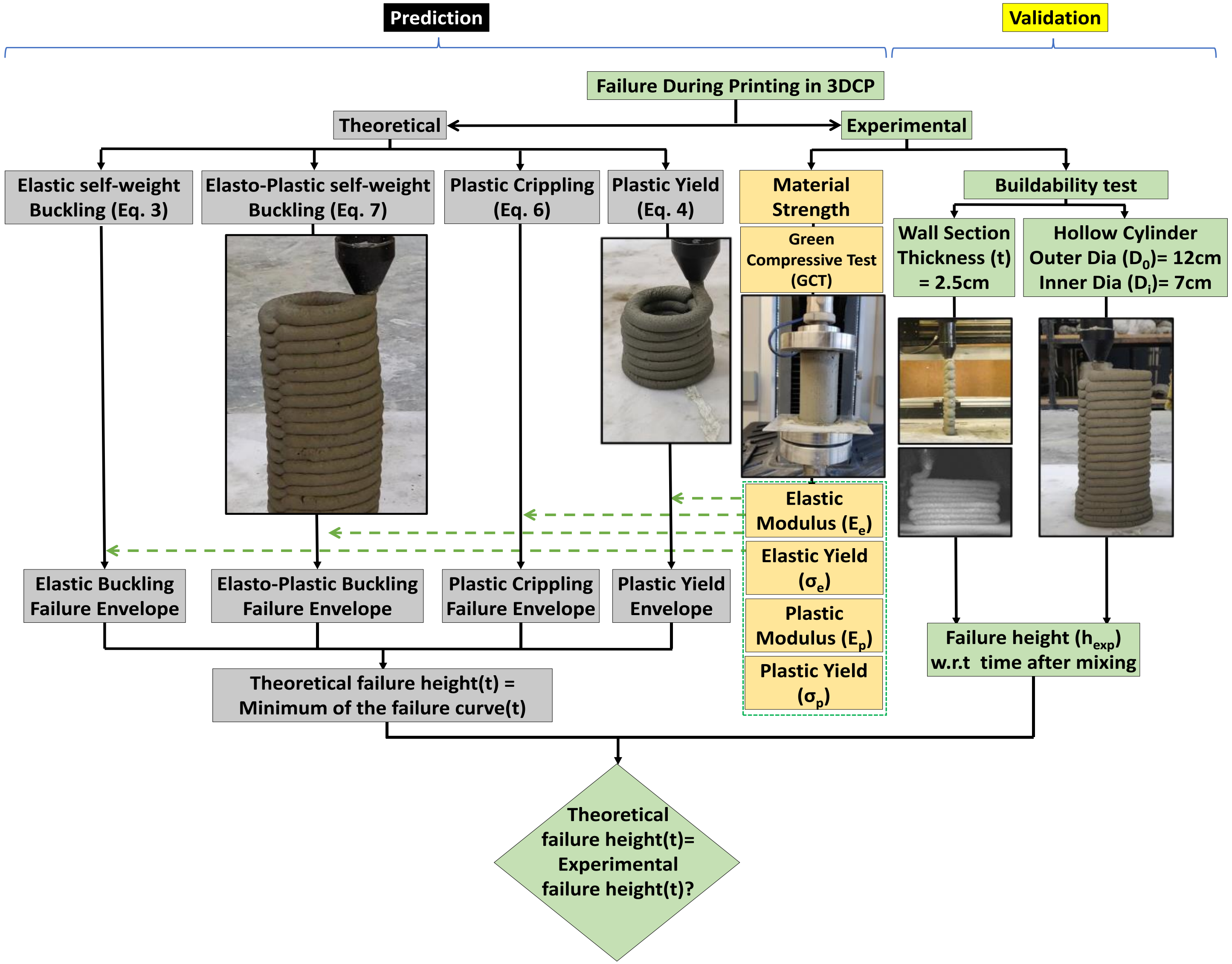


$$h_{b,el} = \left[7.8373 \frac{E_e I}{\rho g A}\right]^{\frac{1}{3}}$$

$$h_p = \frac{\sigma_p}{\rho g} + h_l$$

$$l_{crip} = \sqrt{\frac{\pi^2 E_p I}{4 \times \sigma_e A}}$$

$$h_{crip} = l_{crip} + h_e$$

$$h_{b,eff} = \left[7.8373 \frac{E_{eff} I}{\rho g A}\right]^{\frac{1}{3}}$$

# Mixtures

| Mixture ID | Mass fraction of ingredients* | | | | | Water-to- binder ratio (w/b) by mass | SP to powder ratio (SP%) by mass | Particle volume fraction in the paste phase |
|---|---|---|---|---|---|---|---|---|
| | OPC | Limestone (L; $d_{50}$=1.5μm) | Fly Ash (F) | Sand (M) | LWA | | | |
| $L_{30\text{-}M}$ | 0.37 (638.30) | 0.16 (273.56) | - | 0.47 (808.51) | - | 0.43 | - | 0.437 |
| $L_{30\text{-}S\text{-}M}$ | 0.37 (688.52) | 0.16 (295.08) | - | 0.47 (872.13) | - | 0.35 | 0.35 | 0.488 |
| $F_{20}L_{10\text{-}M}$ | 0.36 (646.00) | 0.05 (92.28) | 0.10 (184.56) | 0.49 (875.88) | - | 0.37 | - | 0.491 |
| $L_{30\text{-}LWA}$ | 0.49 (688.52) | 0.21 (295.08) | - | - | 0.30 (424.59) | 0.35 | 0.25 | 0.488 |

*Values in parenthesis represent the amounts of ingredients in kg/$m^3$

# Experiments

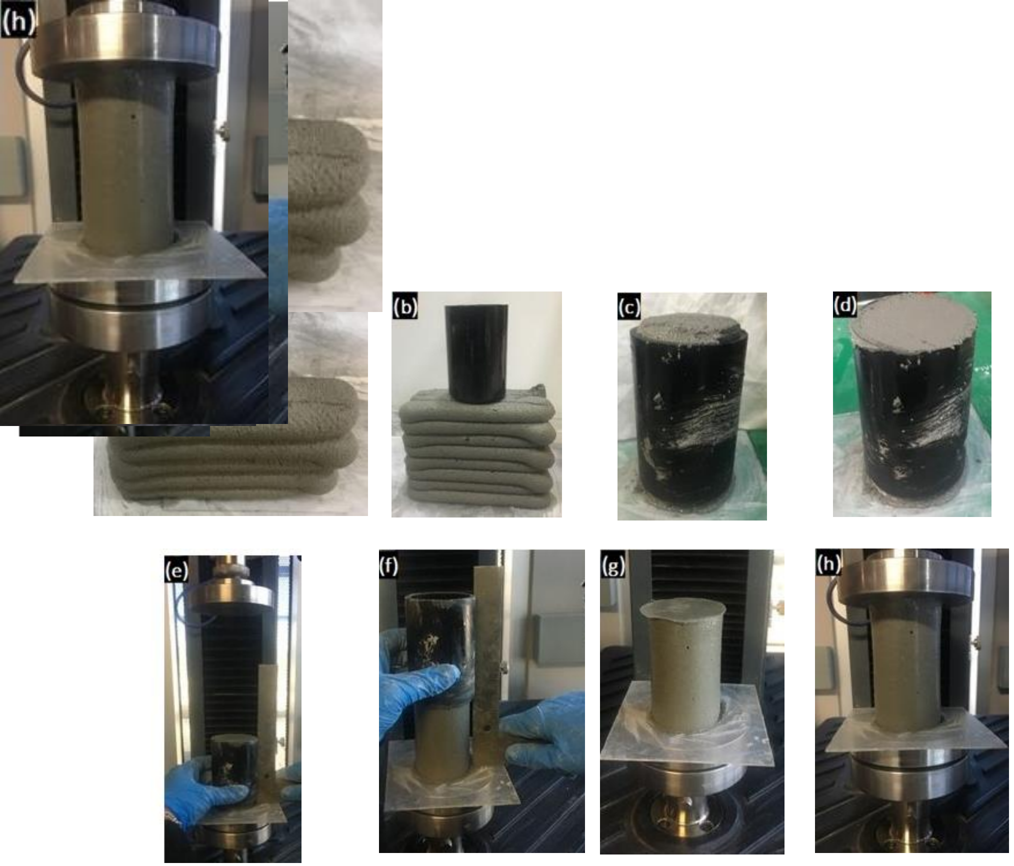


- Green compression test (stress-strain, at very low rates)
- Extract elastic and plastic stresses and moduli
- Predict different failure heights

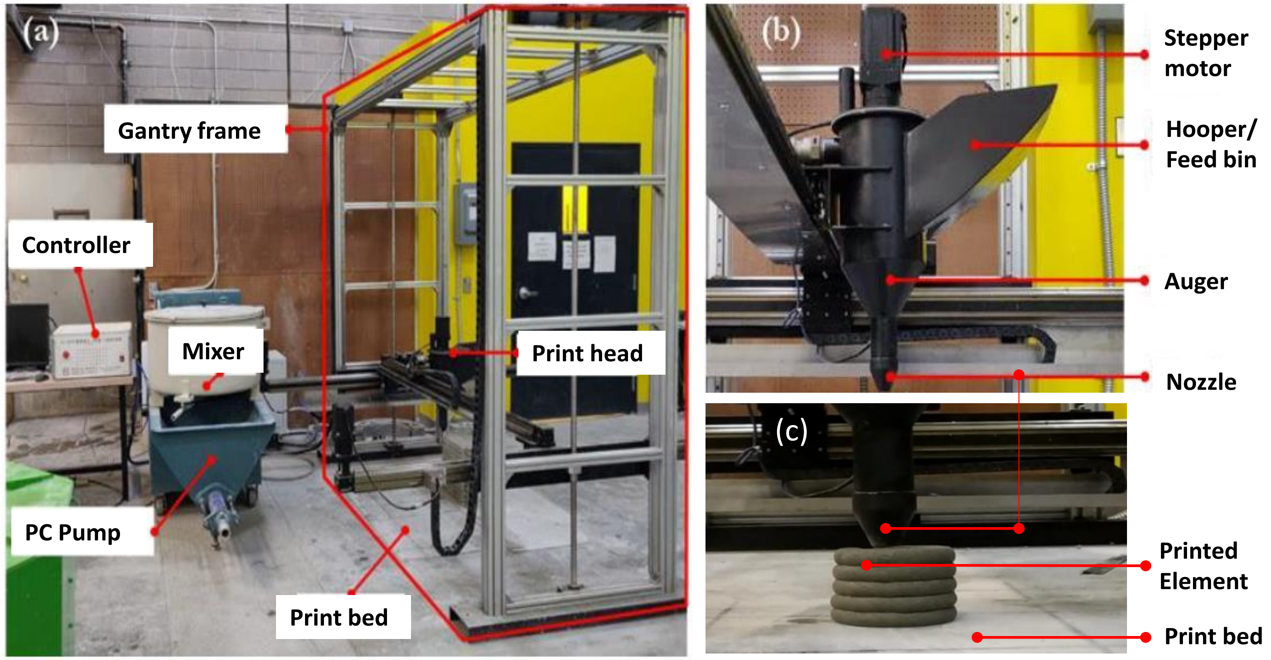


- Print wall and hollow cylinder samples at different times
- Compare experimental height of failure to those predicted using different models of failure

Arizona State University

# Fresh state parameters

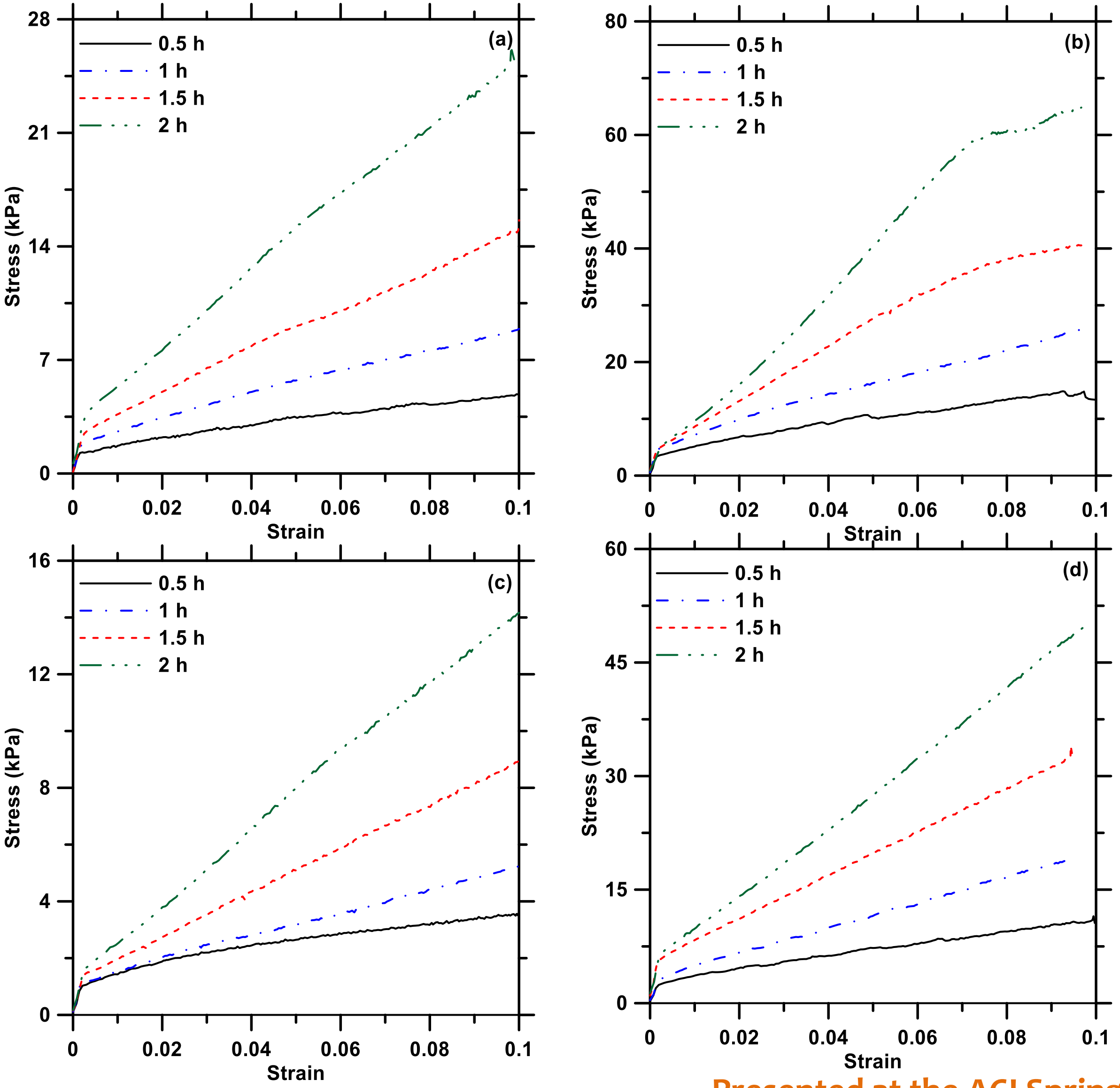


| Mixture ID | Time (h) | Elastic | | Plastic | |
|---|---|---|---|---|---|
| | | Yield stress (kPa) | Modulus (MPa) | Yield stress (kPa) | Modulus (MPa) |
| $L_{30\text{-}M}$ | 0.5 | 1.21 | 0.99 | 2.28 | 0.056 |
| | 1.0 | 1.65 | 1.03 | 3.58 | 0.088 |
| | 1.5 | 2.56 | 1.14 | 6.74 | 0.14 |
| | 2.0 | 3.71 | 1.47 | 13.10 | 0.22 |
| $L_{30\text{-}S\text{-}M}$ | 0.5 | 3.49 | 2.51 | 6.00 | 0.19 |
| | 1.0 | 4.54 | 3.68 | 9.70 | 0.30 |
| | 1.5 | 4.62 | 3.66 | 25.00 | 0.45 |
| | 2.0 | 4.94 | 2.36 | 48.10 | 0.60 |
| $F_{20}L_{10\text{-}M}$ | 0.5 | 1.06 | 0.57 | 1.98 | 0.047 |
| | 1.0 | 1.06 | 0.69 | 2.20 | 0.055 |
| | 1.5 | 1.38 | 0.64 | 3.91 | 0.074 |
| | 2.0 | 1.61 | 0.68 | 6.57 | 0.12 |
| $L_{30\text{-}LWA}$ | 0.5 | 2.49 | 1.49 | 4.10 | 0.14 |
| | 1.0 | 3.33 | 1.63 | 6.05 | 0.20 |
| | 1.5 | 5.77 | 3.60 | 16.70 | 0.30 |
| | 2.0 | 6.58 | 3.19 | 27.70 | 0.41 |

# Yield stress growth

- The plastic yield stress obtained from GCT can be considered to be related to the shear yield stress of the deposited material (in a manner similar to how extrusional and shear yield stresses are related)

$$\sigma_p(t) = \alpha_{geom} . \tau_0(t)$$

$$\sigma_p(t) = \alpha_{geom} A_{thix} t_c \left(e^{\frac{t}{t_c}} - 1\right) + \sigma_{p,0}$$

$$\sigma_0(t) = A^*_{thix} t_c \left(e^{\frac{t}{t_c}} - 1\right) + \sigma_{p,0}$$

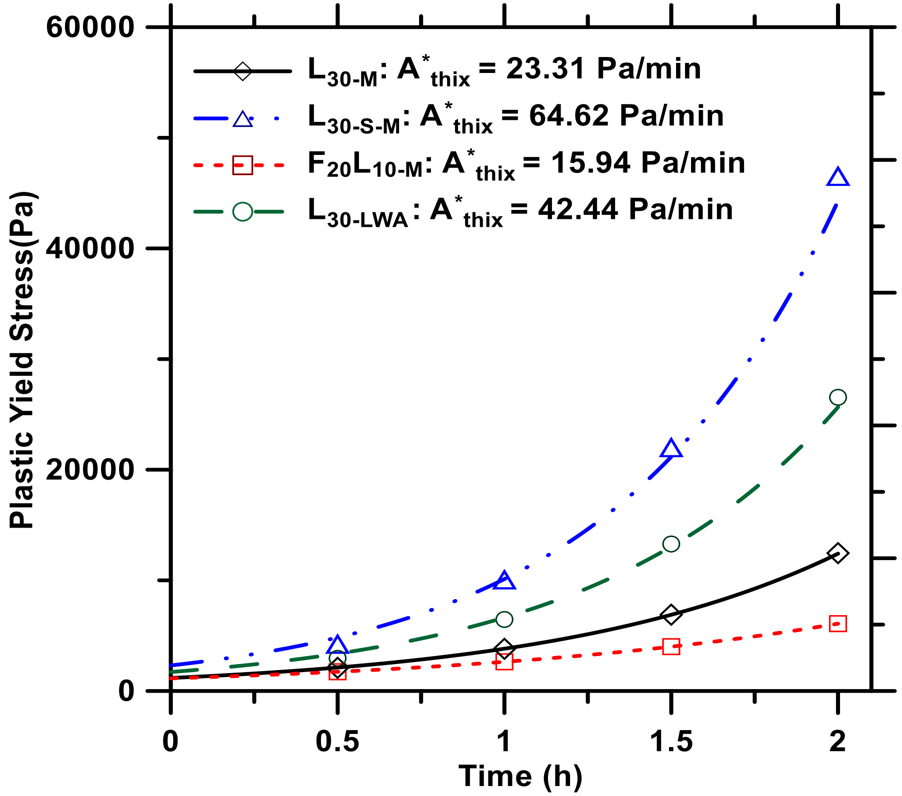

# Model verification

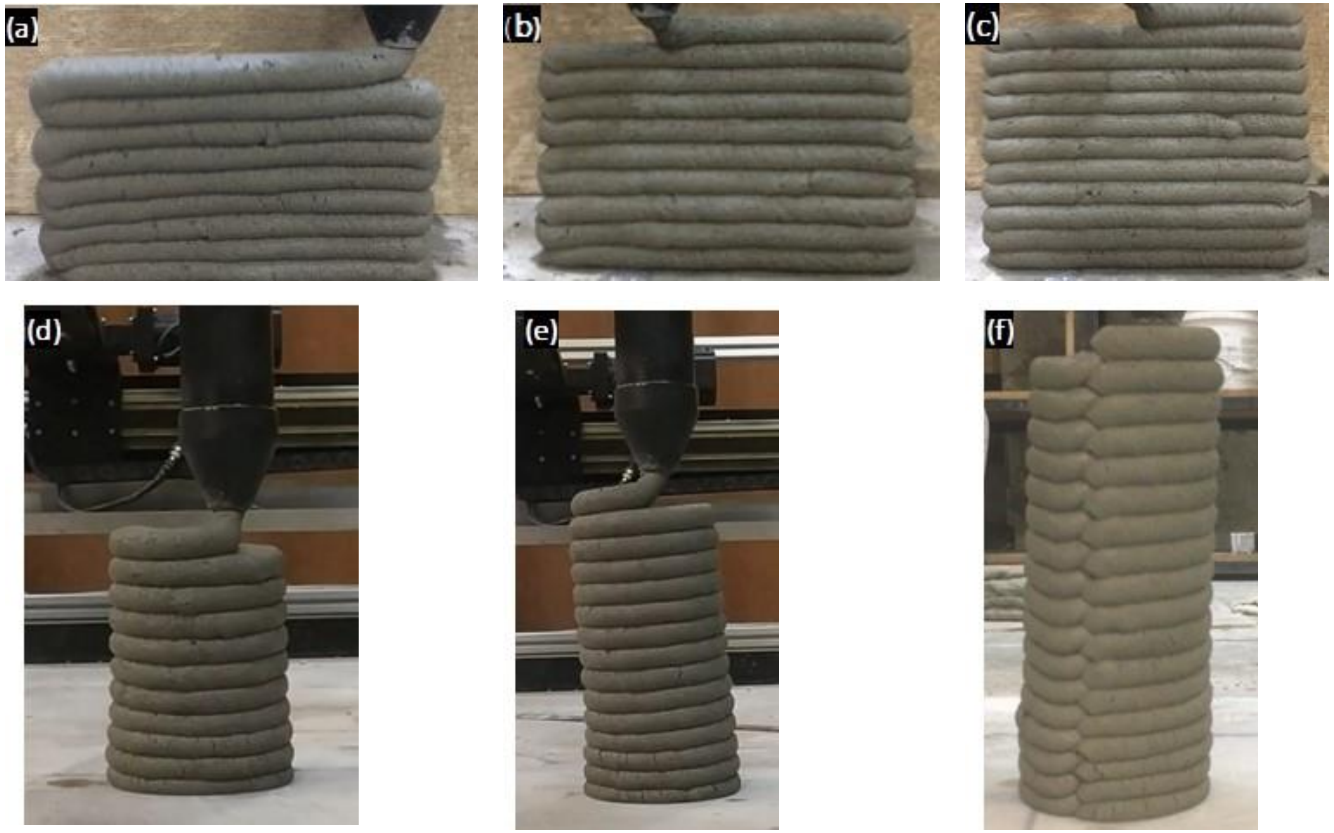


- Failure is defined when no more layers could be printed because of significant geometric deformation and/or collapse of the printed structure
- Wall and hollow cylindrical prints were made every 15 min until 2 h, while the theoretical failure curves are derived from GCT carried out at 30 min intervals until 2 h.

# Buildability predictions

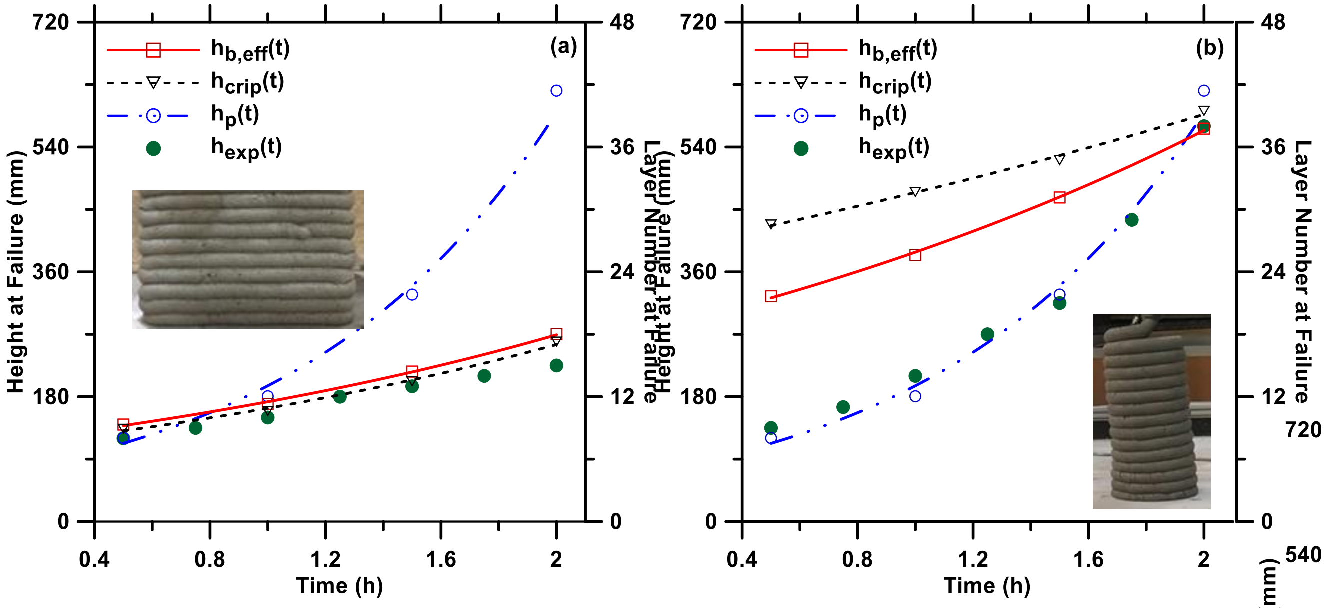


$L_{30\text{-}M}$ mixture

$F_{20}L_{10\text{-}M}$ mixture

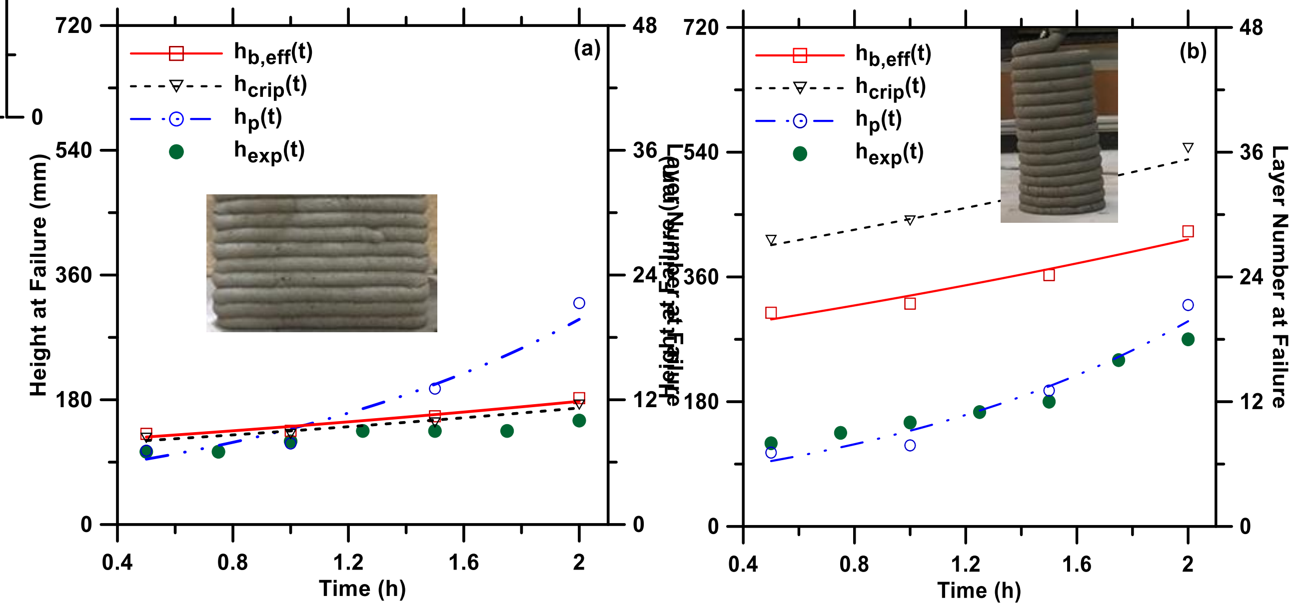

# Observations

- For wall prints, failure heights predicted by buckling/crippling curves < the plastic yield failure for all the print times.
- Plastic failure curve is independent of the print geometry, and scales with the time-dependent plastic yield stress.
- Buckling/crippling failure curves are dependent on the geometry of the section (moment of inertia), along with the modulus.
- For cylinder prints, the failure modes change with time, in some cases, and a cross-over is noticed.
- At the transition points between the multiple failure mechanisms, the experimental cylinder print failure heights are generally lower than the theoretical predictions - attributed to the combined effects of multiple failure modes, causing premature failure.

# Digital image correlation

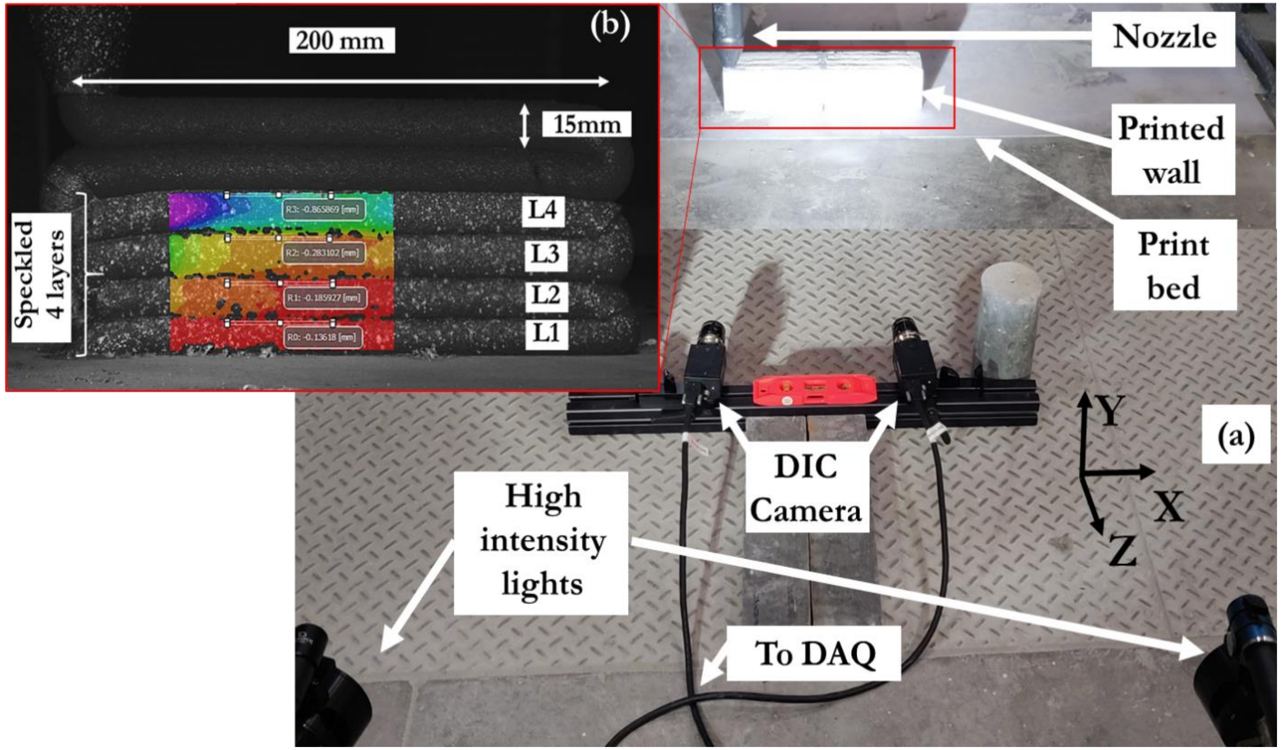


Linear region elements placed near the top of each layer is used to calculate the average vertical displacement of the layers as the printing progresses.

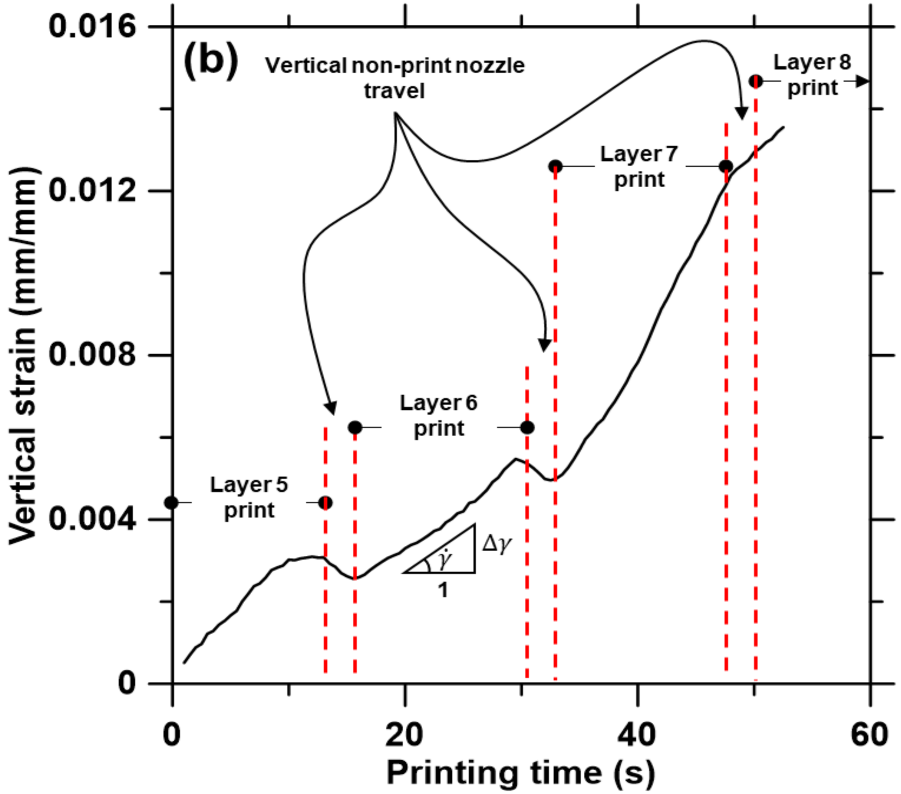


Stepwise strain profile of layer 1 when layers 5, 6, 7, and 8 are printed, showing a linear increase followed by a dip/plateau corresponding to layer shifting

# Displacement profiles

## Vertical displacement

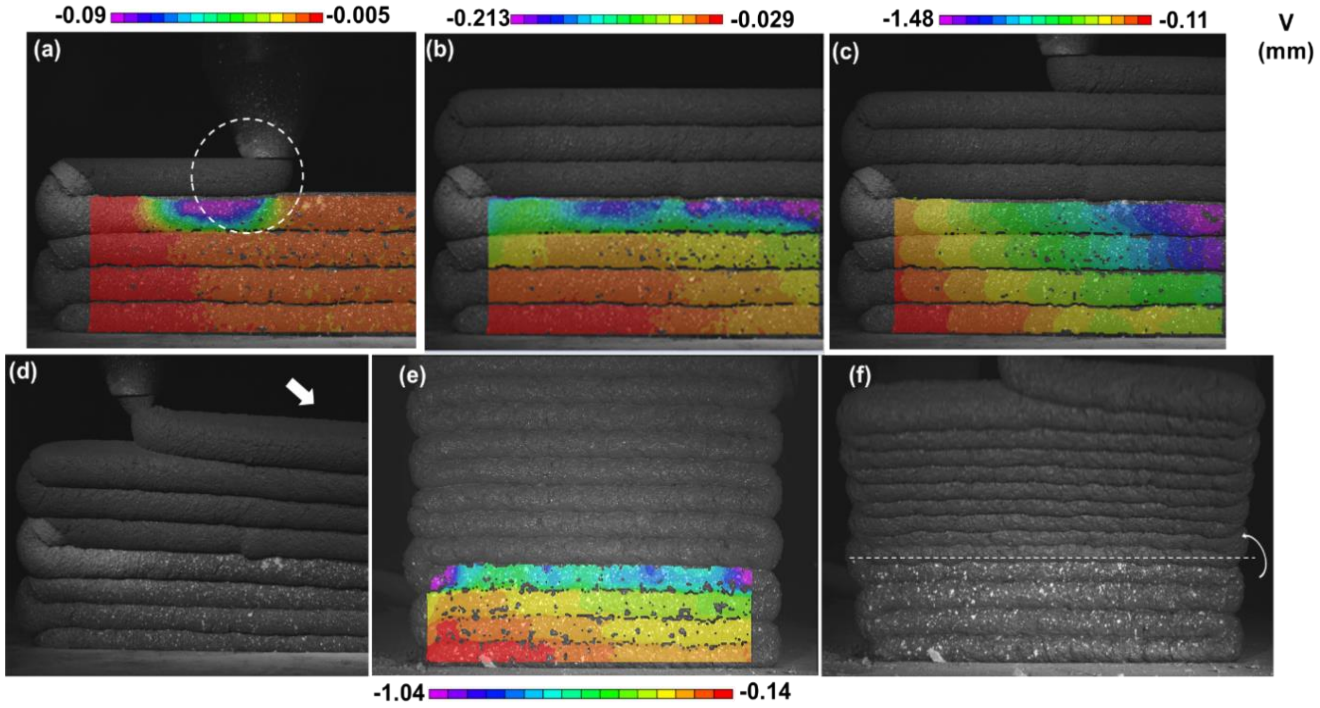


## Out-of-plane displacement

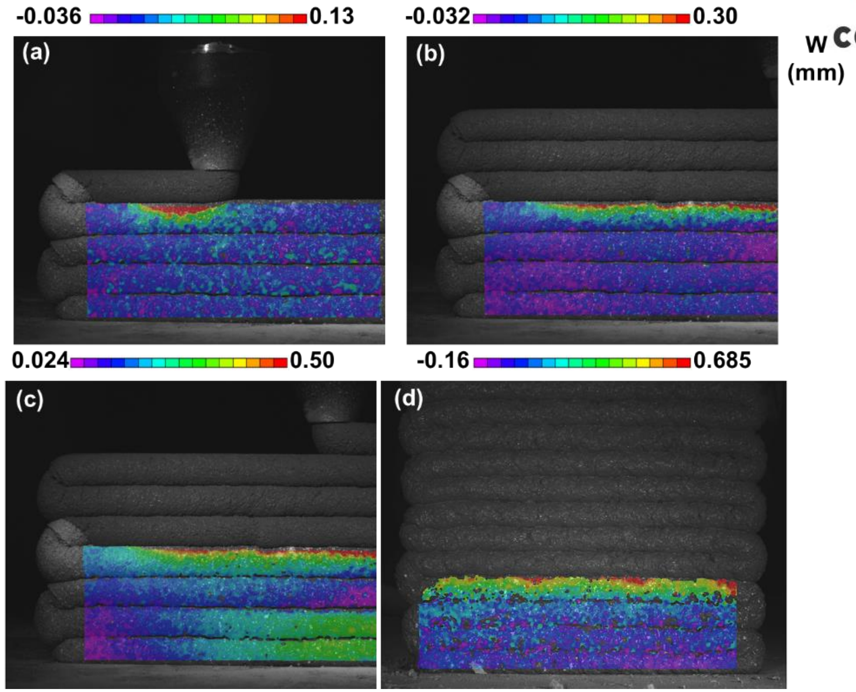


(a) during printing resumed after speckling, (b) 3 additional layers are printed, (c) significant increase in vertical displacement is detected before failure initiation, and (d) at critical failure when right end of the print fails under plastic collapse. Lightweight mortar: (e) right before failure with no specific localized displacement increase after a number of layers are printed, and (f) crippling near the interface of 5$^{th}$ and 6$^{th}$ layers

# Strain rates as failure indicators

- Critical failure height is recorded from the experimental buildability test for wall prints when visible failure (print collapse) occurs.
- Strain rates could be used to indicate failure initiation
  - Consistent increase in slope of the curve, followed by a dramatic increase as further layers are printed - plastic collapse failure
  - A slow increase in slope, followed by a decrease in slope when many layers are printed - buckling or crippling
  - Reduction in strain (or a negative change in strain rate) indicates that the speckled points are moving upwards, and the wall is toppling away from the camera's plane of views, which could occur only in the buckling mode

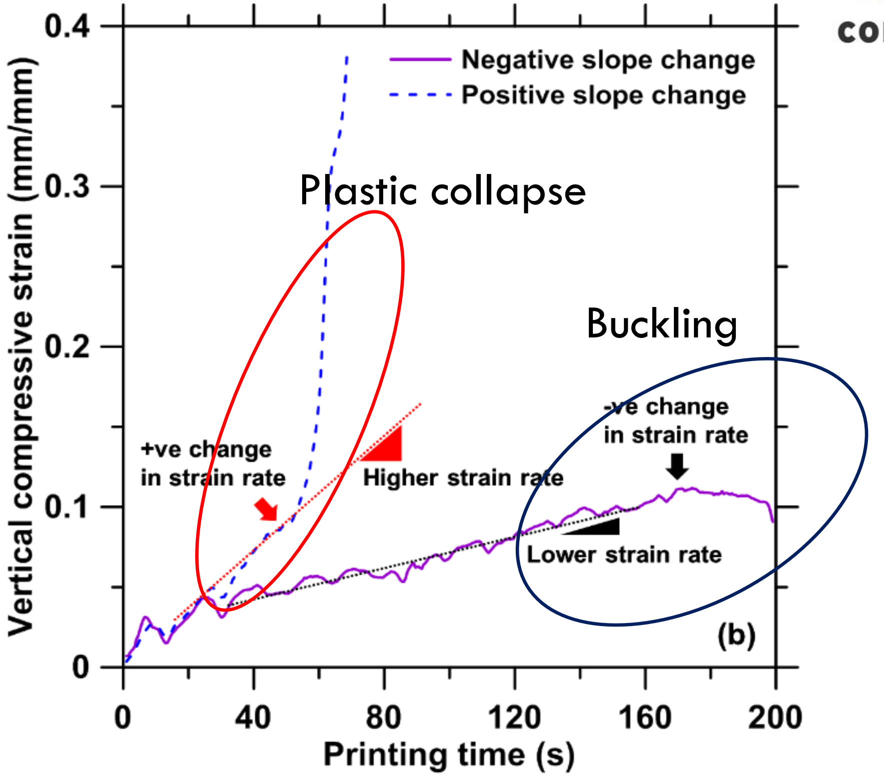


Typical strain profiles characteristic to plastic collapse and buckling failure, based on the calculated changes in strain rate, and vertical compressive strain profiles extracted from layer 2

# Strain-time relations and interpretations

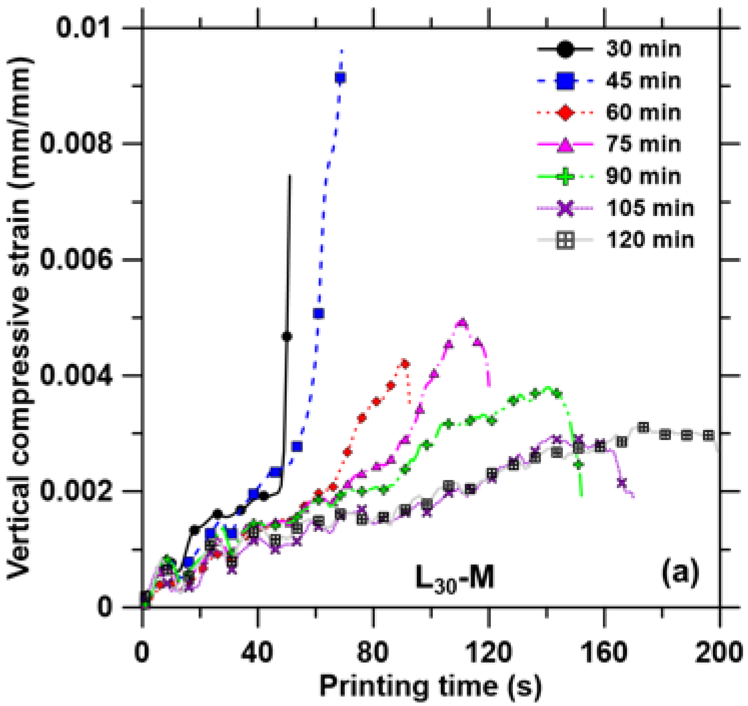


- Time corresponding to the last strain measurement indicates the number of layers
- Change in failure mode with time
- Depends on the mixture and the geometry

# Critical and initiation heights

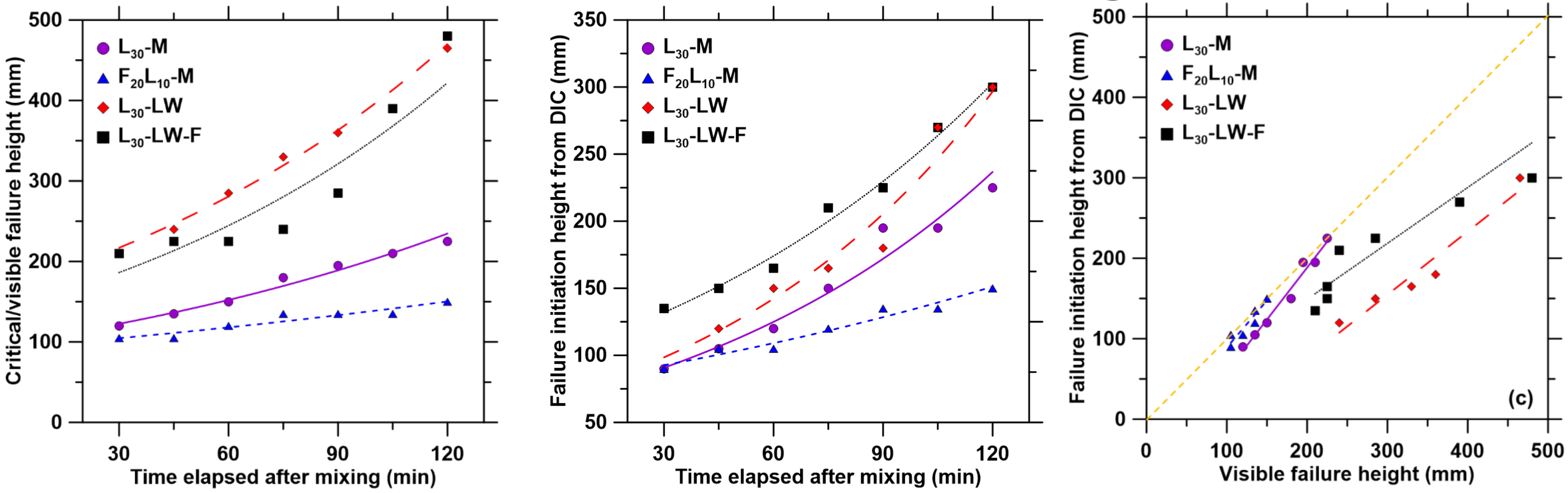


- Similar patterns for critical and initiation heights (initiation height < critical height)
- Lightweight mixtures have significantly different critical and initiation heights
  - Lower superimposed stresses enabling better buildability – stress reduction of ~1 kPa in the bottommost layer after building up 23 layers
  - Better rate of stiffness increase – 3.1 kPa/min (vs. 1.82 kPa/min)

# Failure envelopes

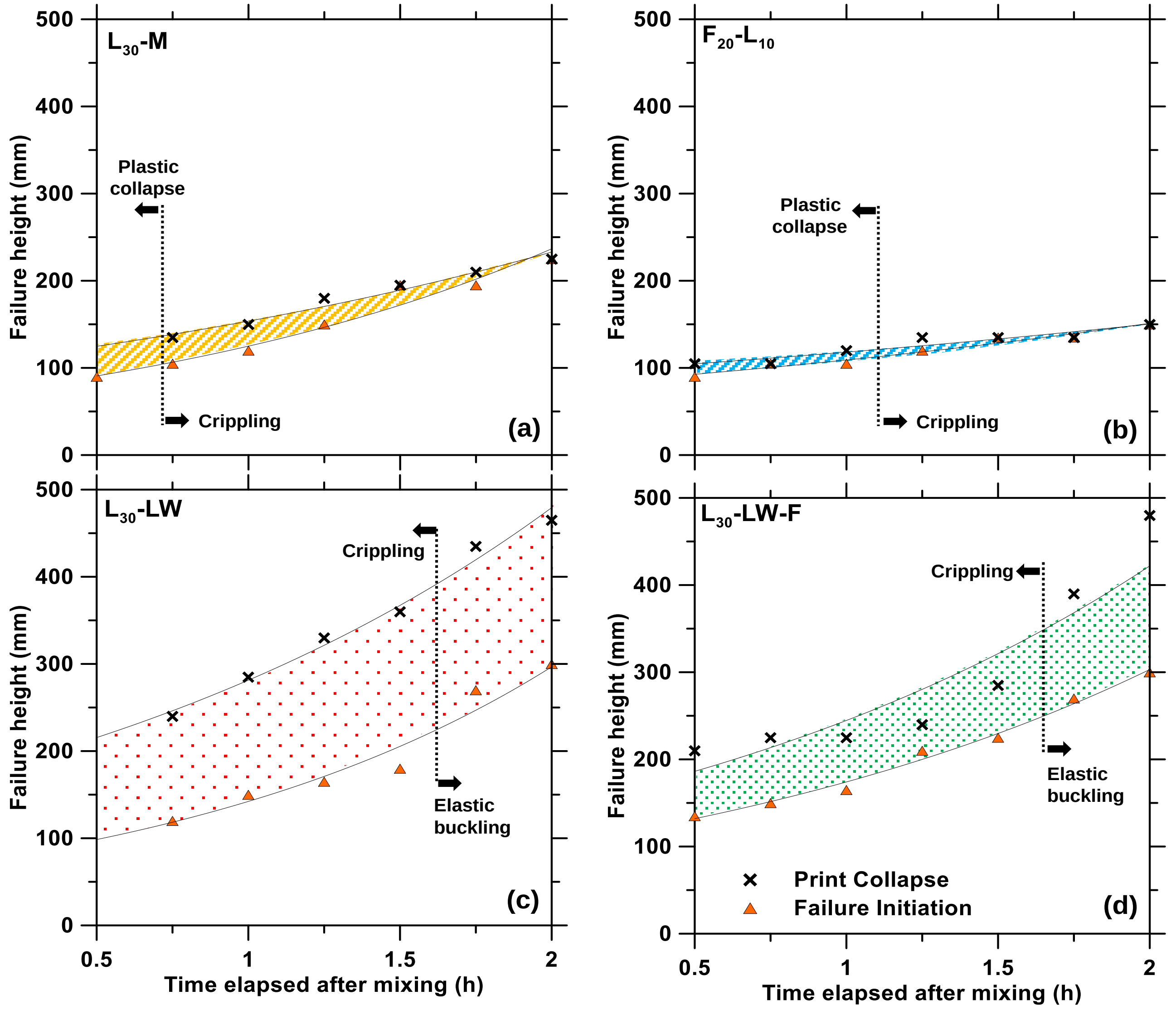


- Elastic collapse corresponds to the limiting elastic yield stress; partial structural buckling (crippling) while the material is soft
- Combination of analytical model and DIC results
- Shaded regions show the additional height that the wall could be built before visual collapse after failure initiation had been detected using DIC
- Lightweight mixtures show a larger zone

# Conclusions

- Analytical model accounting for failure mechanisms to predict buildability – easily standardized
- An approach based on cumulative vertical strains to indicate buildability of chosen mortar mixtures
- DIC identified plastic collapse and buckling/crippling of the printed structure using strain profiles
- Vertical strain build-up rate indicative of the stiffness development when printed at different times, thereby positioning DIC as a real-time method to monitor relative material property changes.
- Vertical strain profiles can provide decent indications of failure heights and failure modes, however buckling failure prediction from in-plane strains is rather subjective.

# Thank You

# This work was supported by NSF

Narayanan.Neithalath@asu.edu